Measurements of Mass and Z

K.E. Rehm,

Argonne National Laboratory, Physics Division

Mass determination

- Time-of flight technique
- Magnetic rigidity technique
- Recoil mass separator

Time-of-flight techniques:

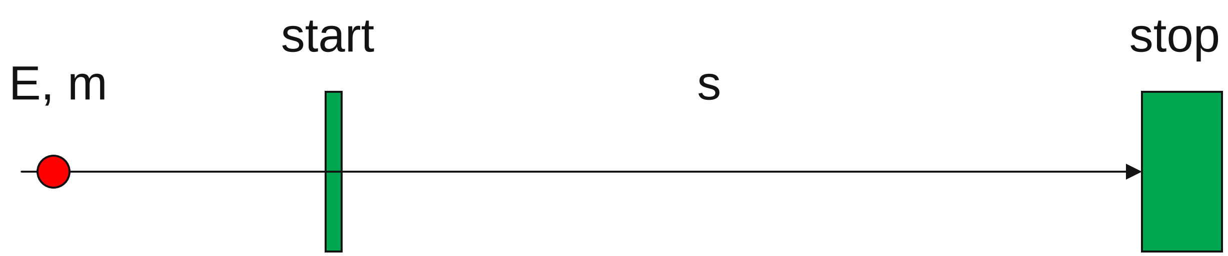

- Thin (homogeneous) Si detector
- C-foil + channel plate detector
- Parallel plate avalanche detector
- No start detector (pulsed beam)

$E = m/2\,(s/t)^2 \rightarrow m \sim Et^2$

$\Delta m/m = \Delta E/E + 2\,\Delta t/t$

Large t (large s, but small $\Delta\Omega$)

TOF spectrum

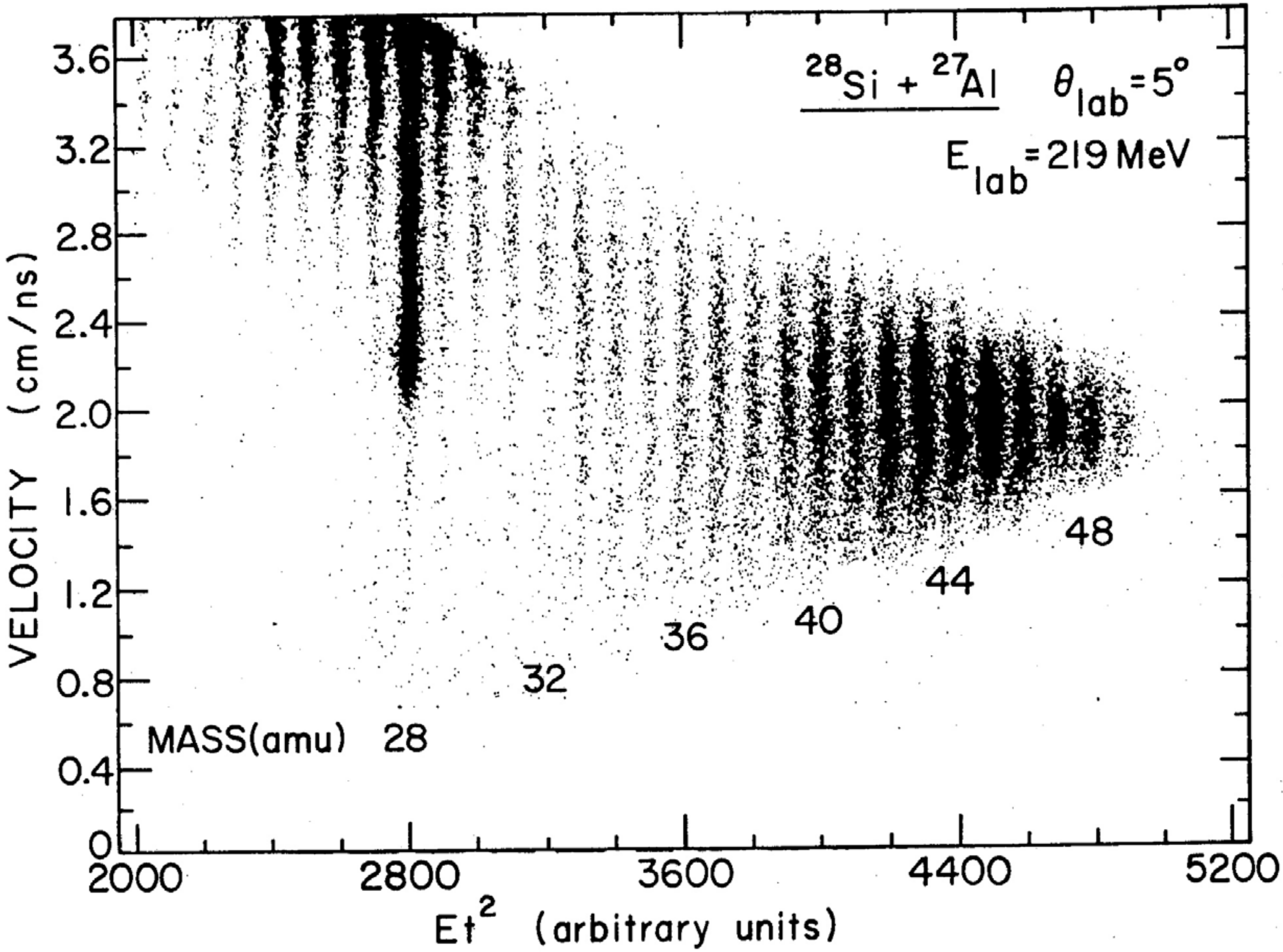

Usually the time resolution limits the mass resolution:

$$\Delta M/M = 2 * \Delta t/t + \Delta E/E.$$

Sometimes (e.g. for very low energy particles, where t is large) $\Delta E/E$ can be the dominant factor.

Standard ionization chamber

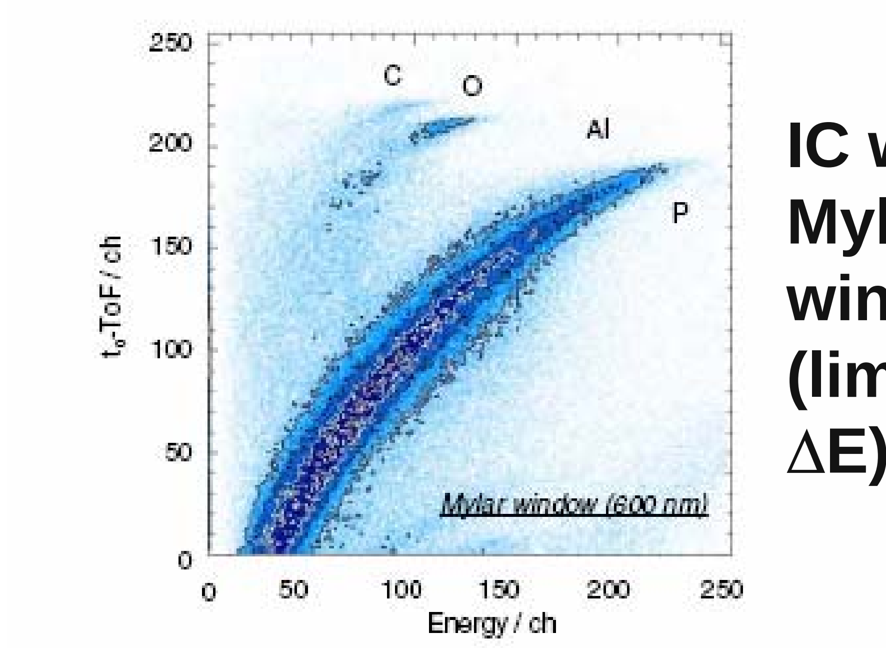

IC with Mylar window (lim. by ΔE)

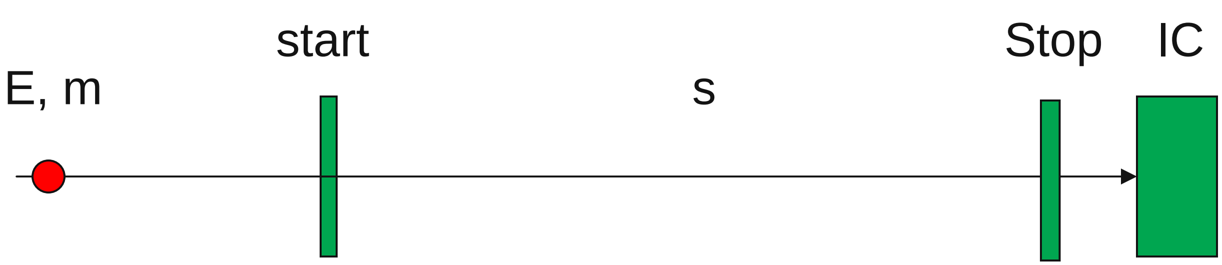

New materials:

SiN with extreme homogeneity

NIMB 248, 155(2006)

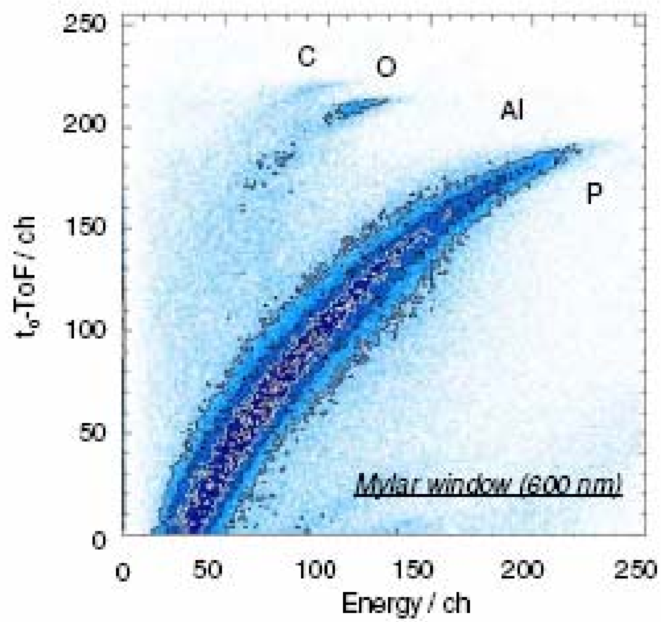

IC with Mylar window

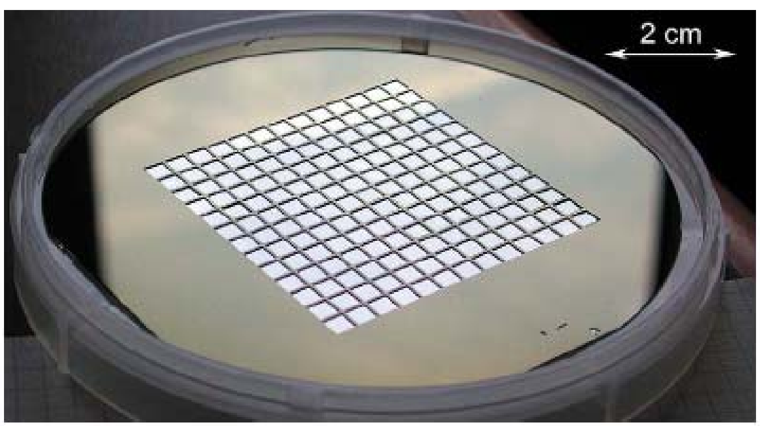

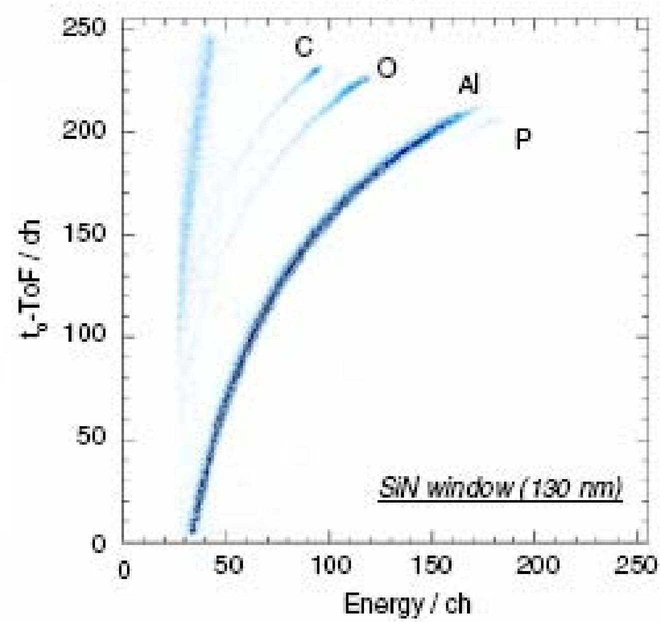

IC with SiN window

Energy (TOF) straggling in SiN (compared to 15 $\mu g/cm^2$ C)

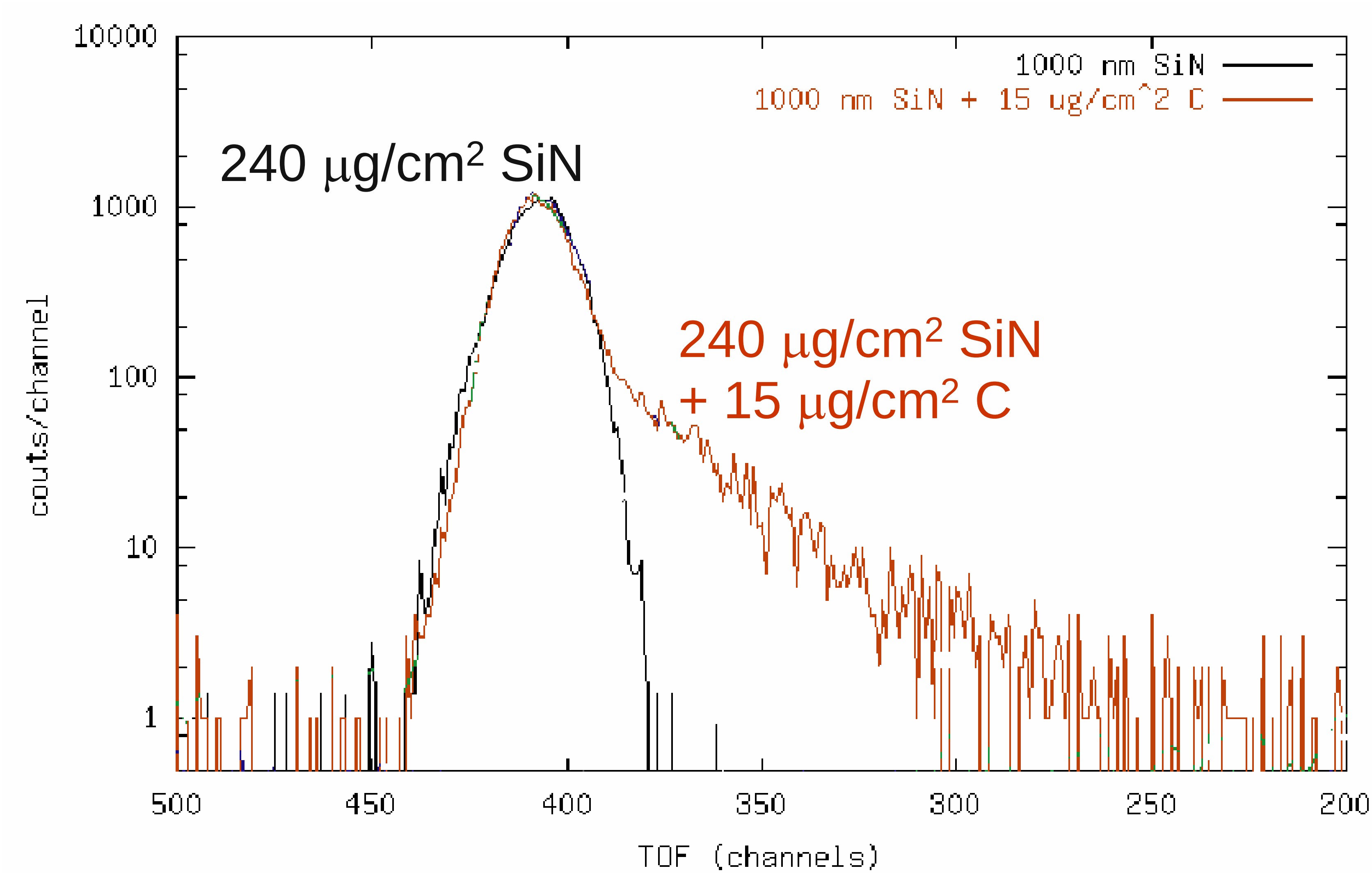

Separation of ^{36}Cl and ^{36}S isobars, used for isobar separation in accelerator mass spectrometry.

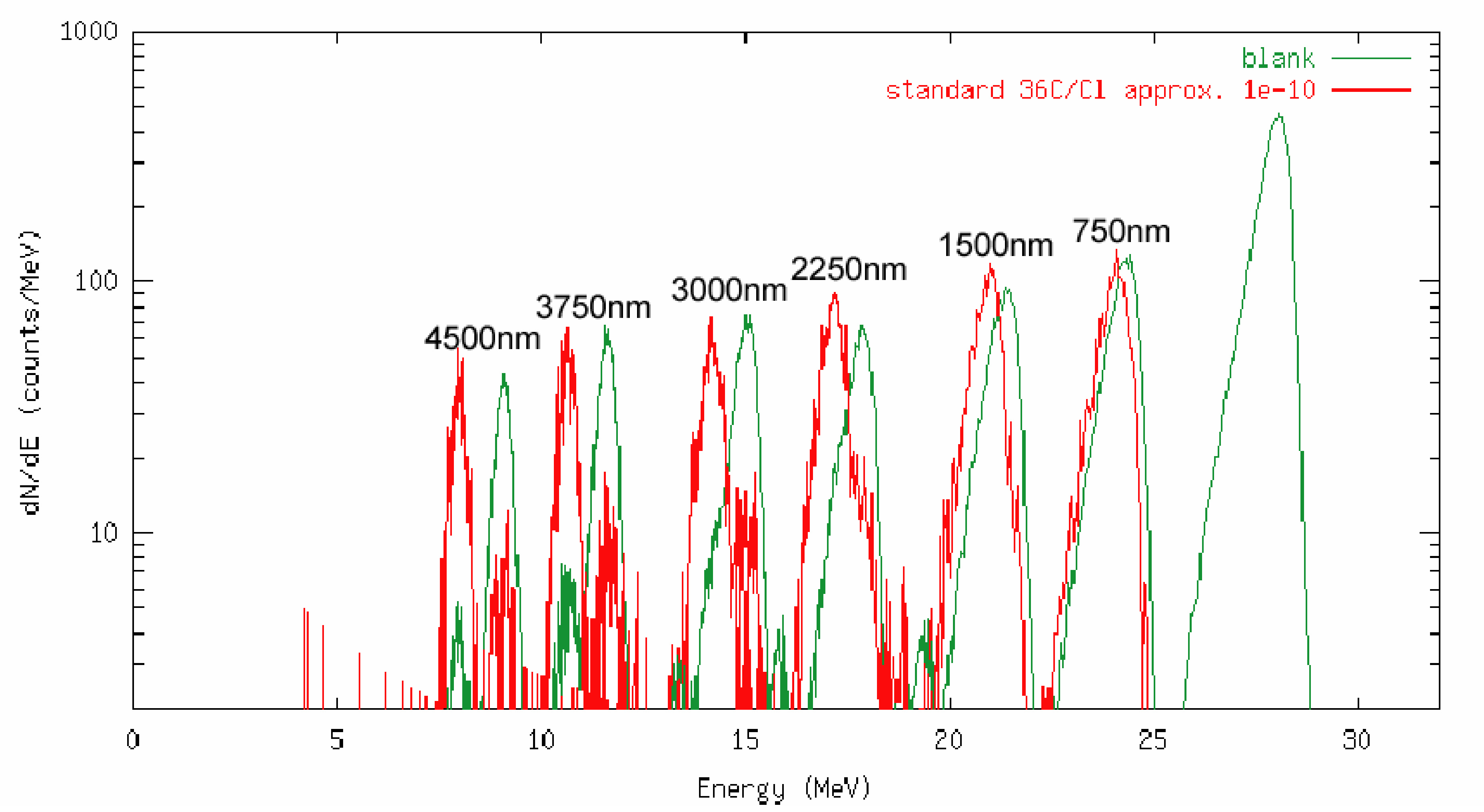

Magnetic rigidity technique:

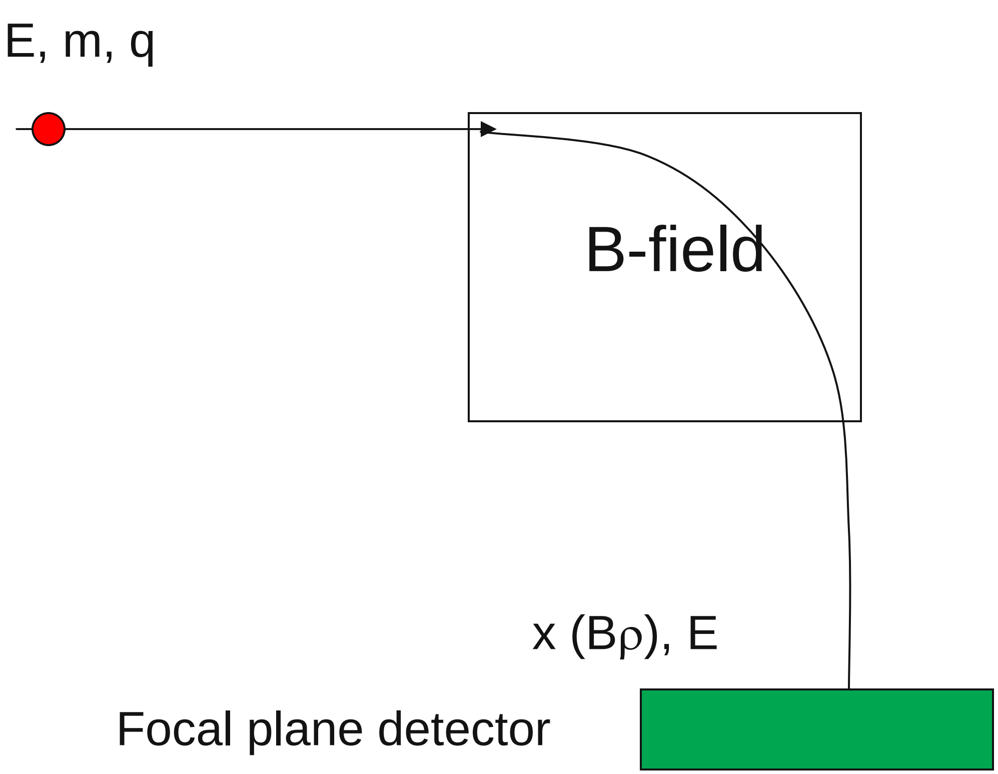

$E = p^2/(2m)$

$B\rho = p/q$

$E = q^2/(2m) \; (B\rho)^2$

Plot E vs $(B\rho)$

Quantized curvature

Example of magnetic rigidity with SPS

$^{208}Pb+^{28}Si$

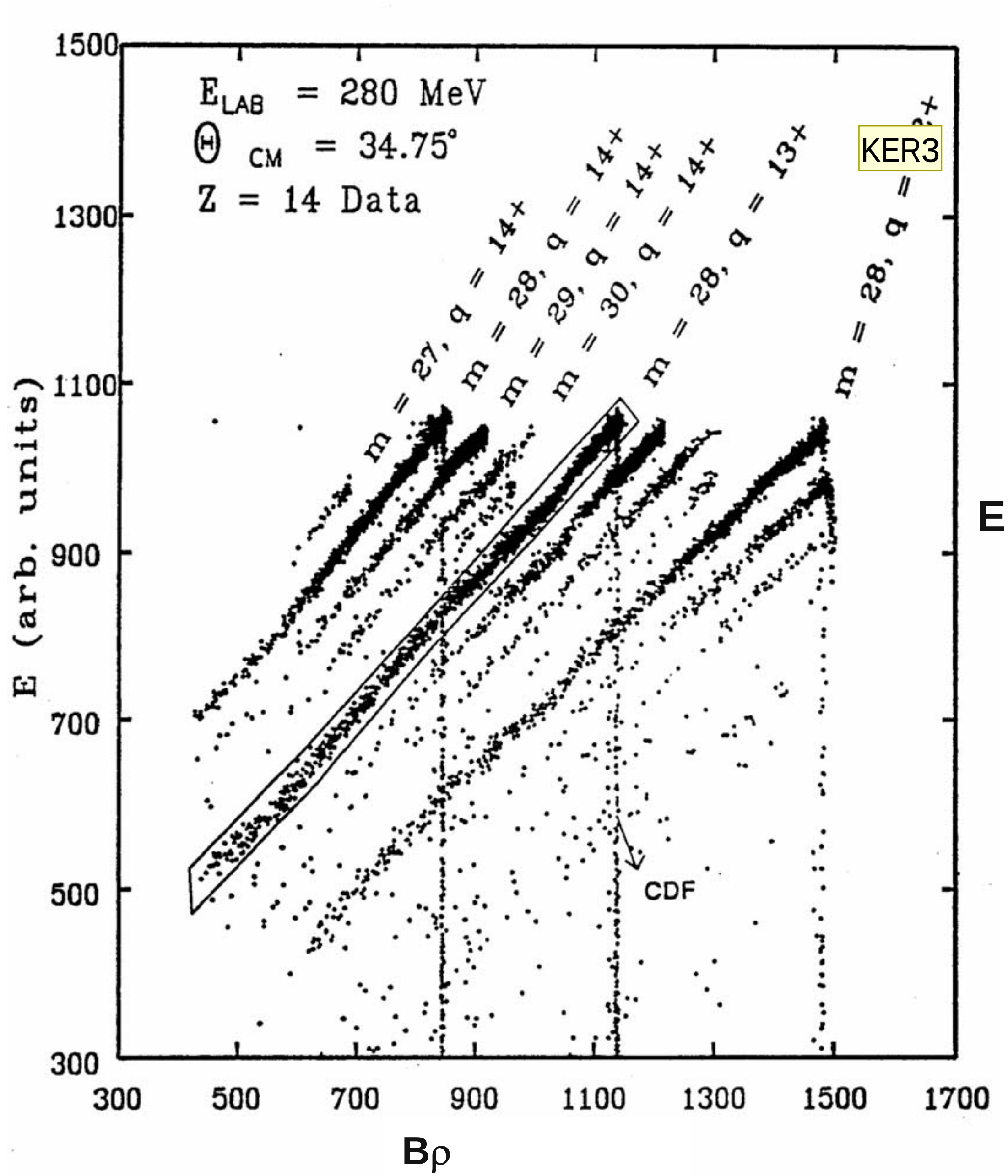

$E=q^2/(2m)*(B\rho)^2$

Slide 13

KER3 rehm, 2/12/2008

Advantages/disadvantages of the magnetic rigidity technique

+ No timing signals needed

- Spectrographs are large

- Possible ambiguities in $q^2/2m$

Recoil mass separators:

Principle of recoil mass separators

Electric fields bend particles ~$E/q = m/q\ v^2/2$

Magnetic fields bend particles ~ $p/q = m/q\ v$

By combining electric and magnetic fields the velocity can be eliminated, resulting in an m/q spectrum in the focal plane.

See H. Enge NIMA 186, 413

Example: Fragment Mass Analyzer (FMA) at Argonne

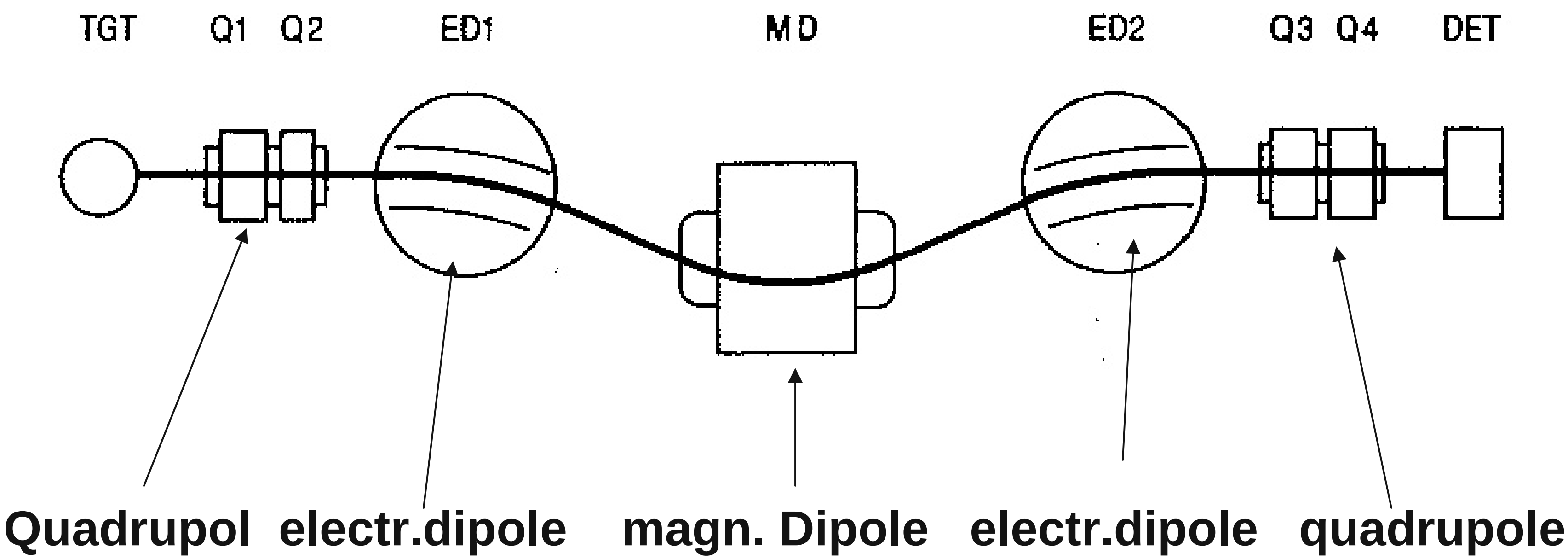

Recoil Mass Separators

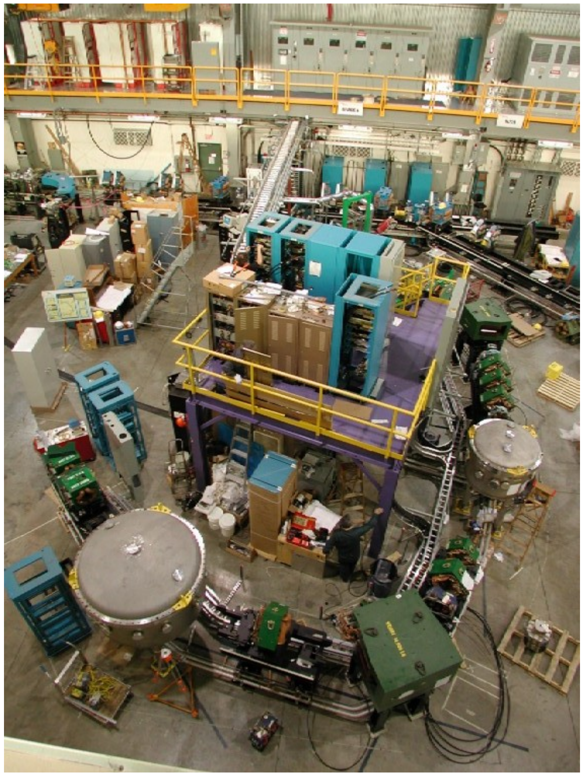

Dragon at TRIUMF

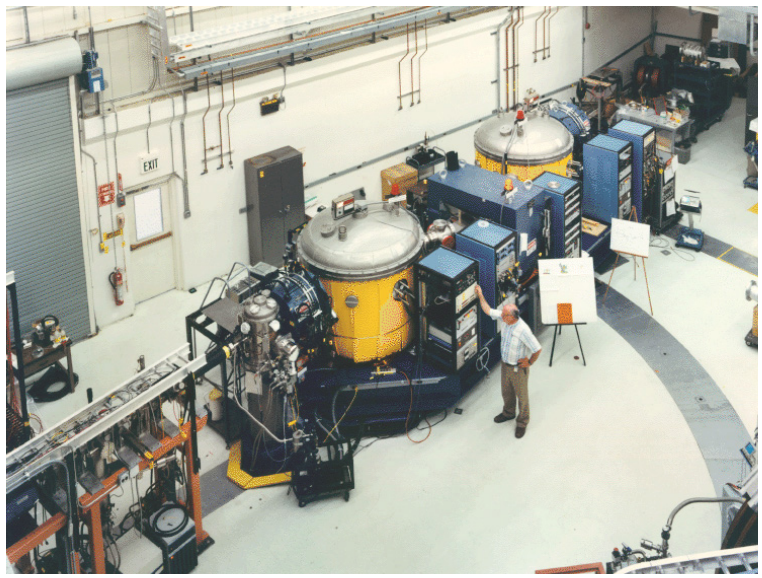

FMA at ATLAS

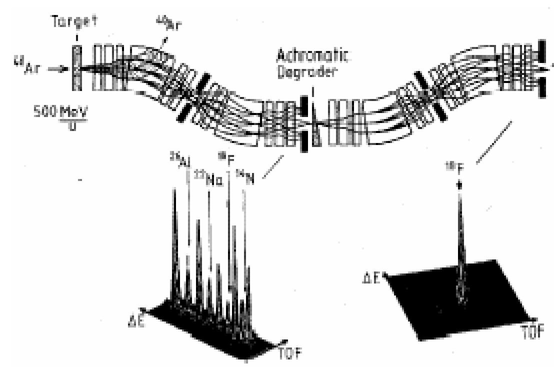

FRS at GSI

Example of m/q ambiguity

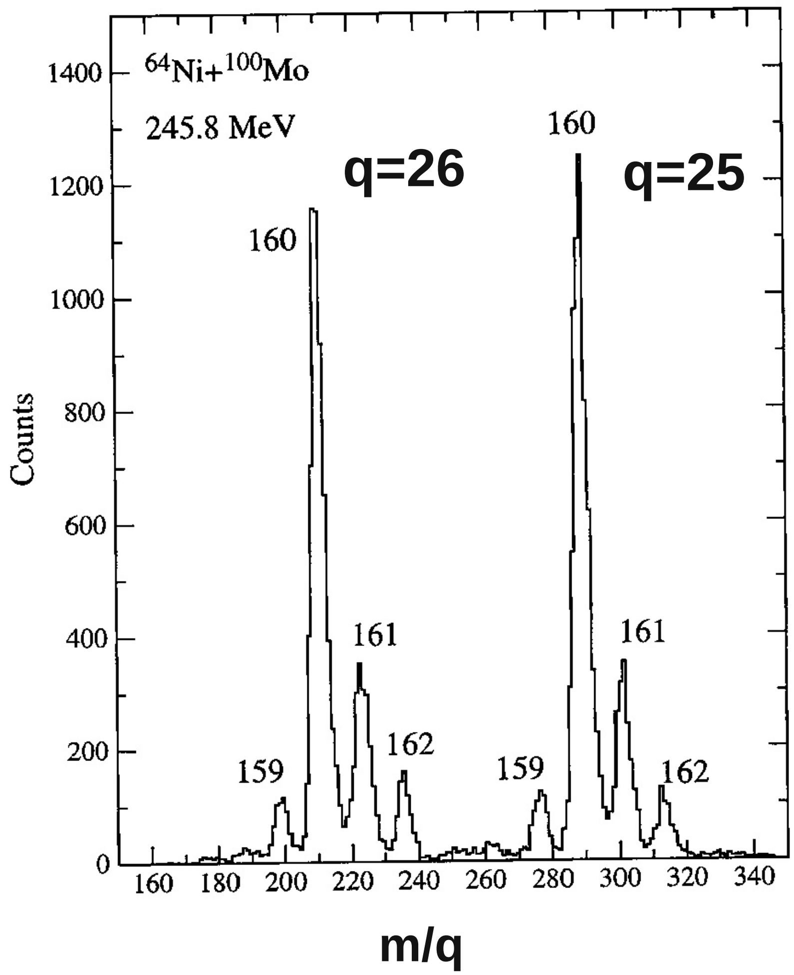

Fusion evaporation ^{64}Ni + ^{100}Mo

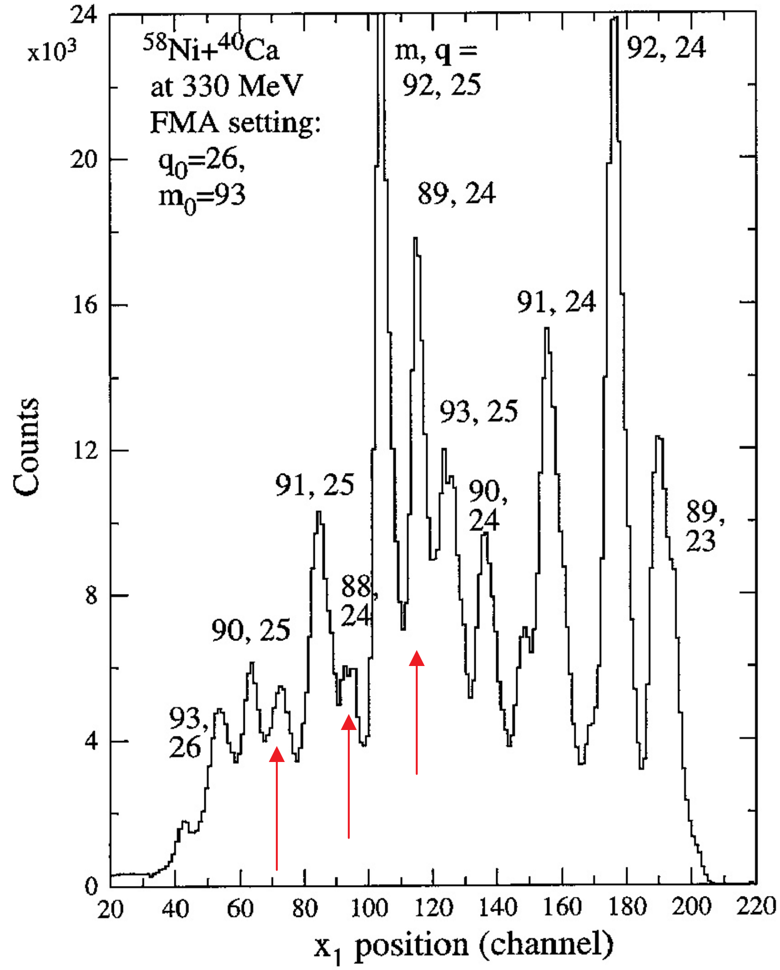

Fusion evaporation ^{58}Ni + ^{40}Ca

Separation of the m/q ambiguity by TOF

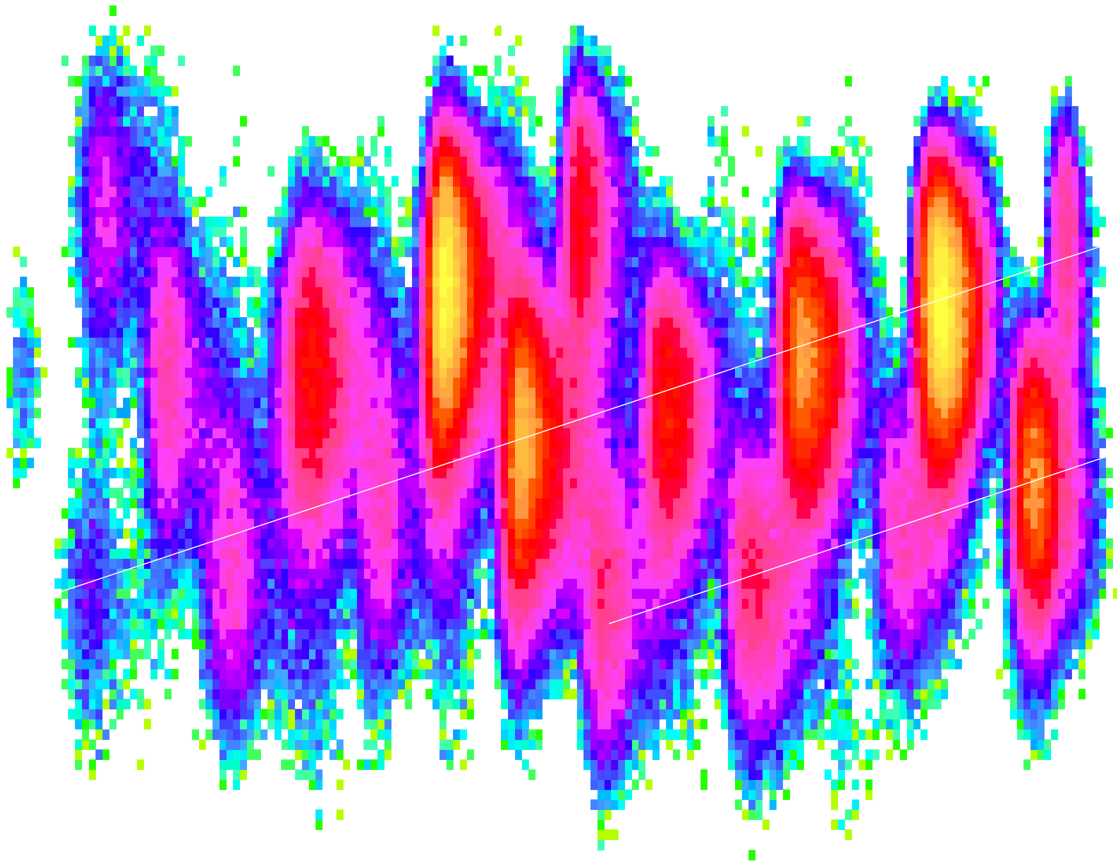

Advantages/disadvantages of recoil separators

+ Excellent mass separation

+ good separation of incident beam

- Large and expensive

- Limited in energy by E/q <10 MeV/u

- m/q ambiguities

Mass measurements with axial - symmetric magnetic fields

HELIOS spectrometer

Inverse kinematics

Measured quantities

Flight time: $T_{flight}=T_{cyc}$

Position: z

Energy: E_{lab}

Derived quantities

Part. ID: m/q

Energy: E_{cm}

Angle: θ_{cm}

Field: 3 Tesla	
Particle	**T_{cyc} (ns)**
p	**21.8**
d,α	**43.6**
t	**65.7**
^{3}He	**32.8**

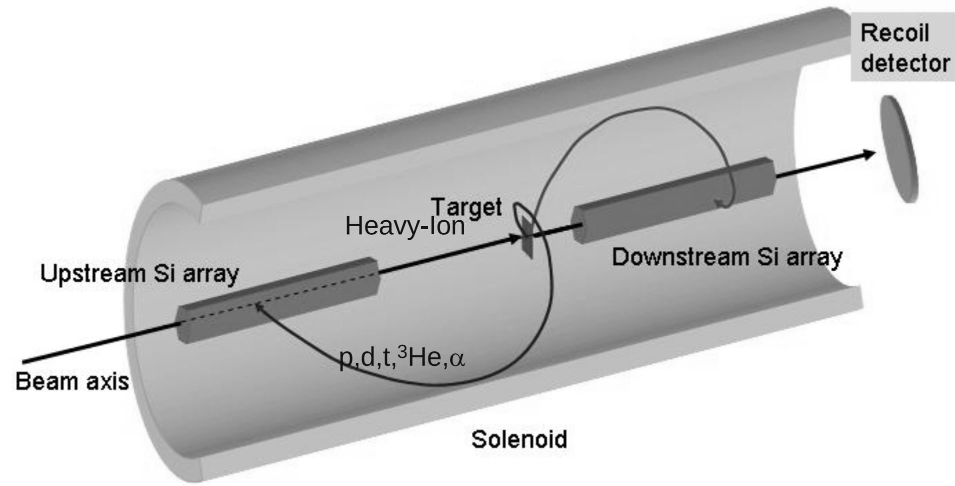

$$\frac{m}{q} = \frac{eB}{2\pi} \times T_{flight}$$

$$E_{cm} = E_{lab} + \tfrac{1}{2} m V_{cm}^2 - \frac{V_{cm} qeB}{2\pi} z$$

$$\theta_{cm} = \arccos\left(\frac{1}{2\pi} \frac{qeBz - 2\pi m V_{cm}}{\sqrt{2mE_{lab} + m^2 V_{cm}^2 - m V_{cm} qeBz / \pi}} \right)$$

Independent of energy!!

Z-determination

- Energy loss
- Range
- Characteristic X-rays
- Gas-filled magnet technique

Energy loss technique

Energy loss formula (Bohr 1915)

$$\frac{dE}{dx} = const \bullet \rho \frac{Z_{material}}{A_{material}} \bullet \frac{MZ_{ion}^{2}}{E} \bullet f(E)$$

stopping material   ion properties   slowly varying

Example of ΔE-E particle identification

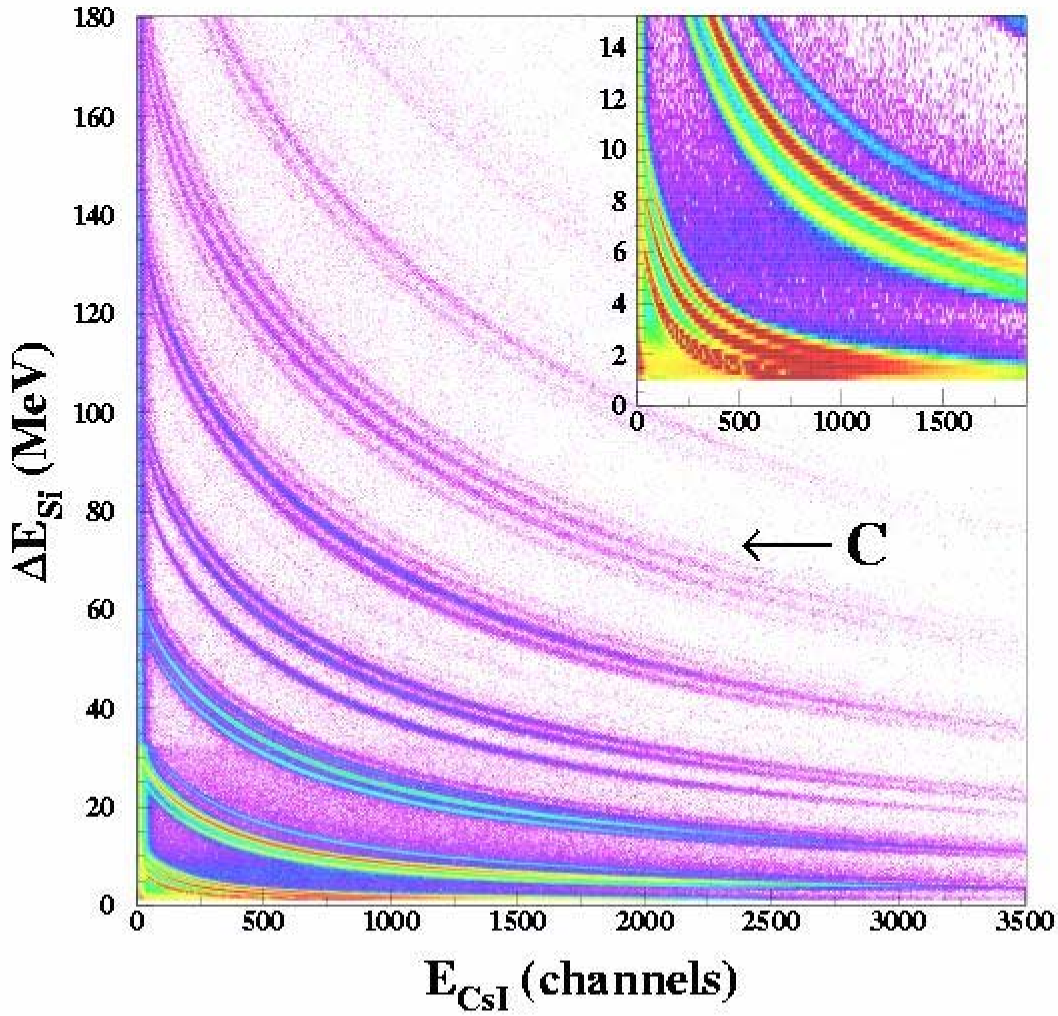

$\Delta E \sim MZ^2/E$

from

Indiana University,
Chemistry Department

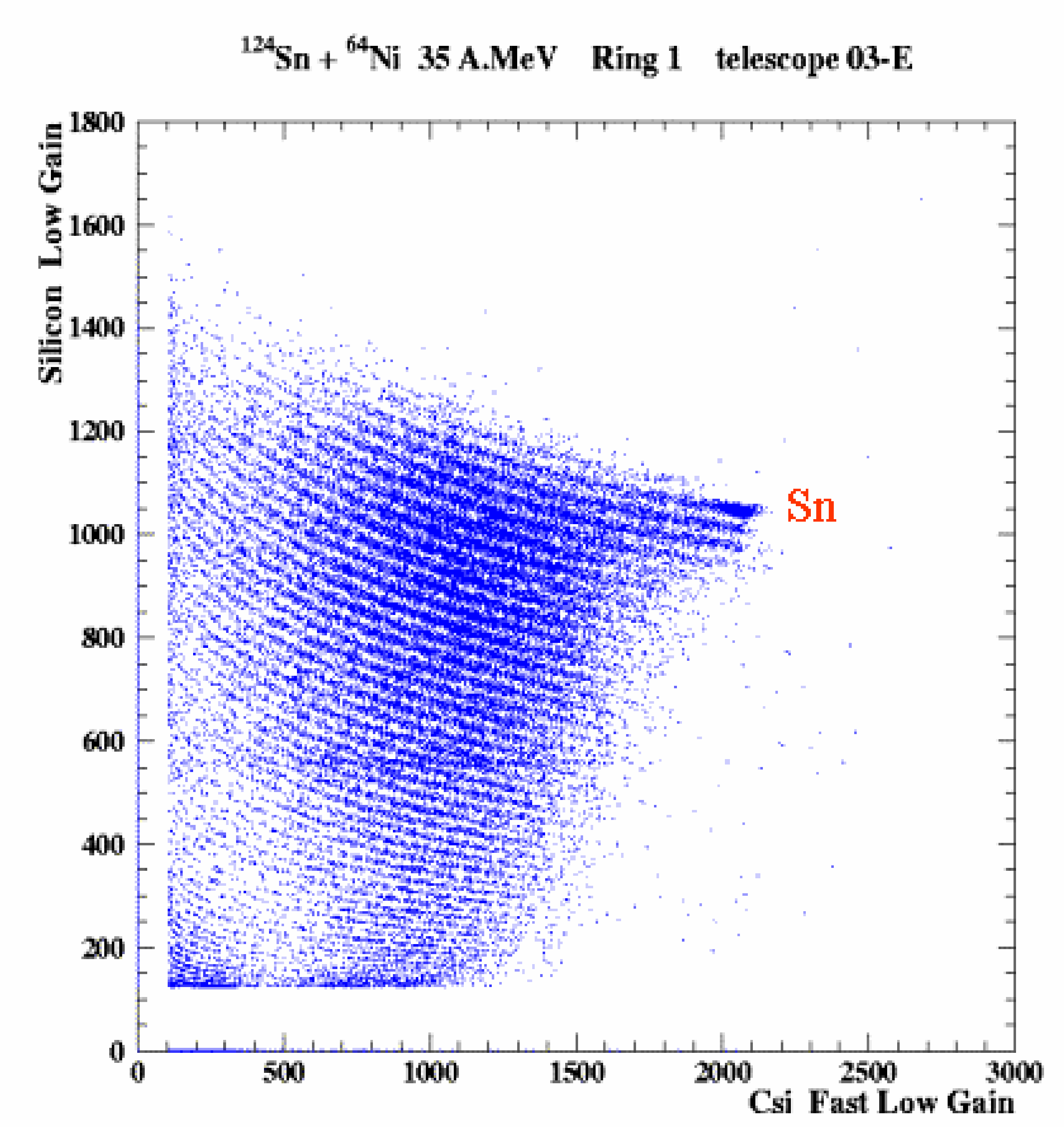

From

Chimera, INFN Catania

230 MeV (5.75 MeV/u) ^{40}Ca on ^{12}C

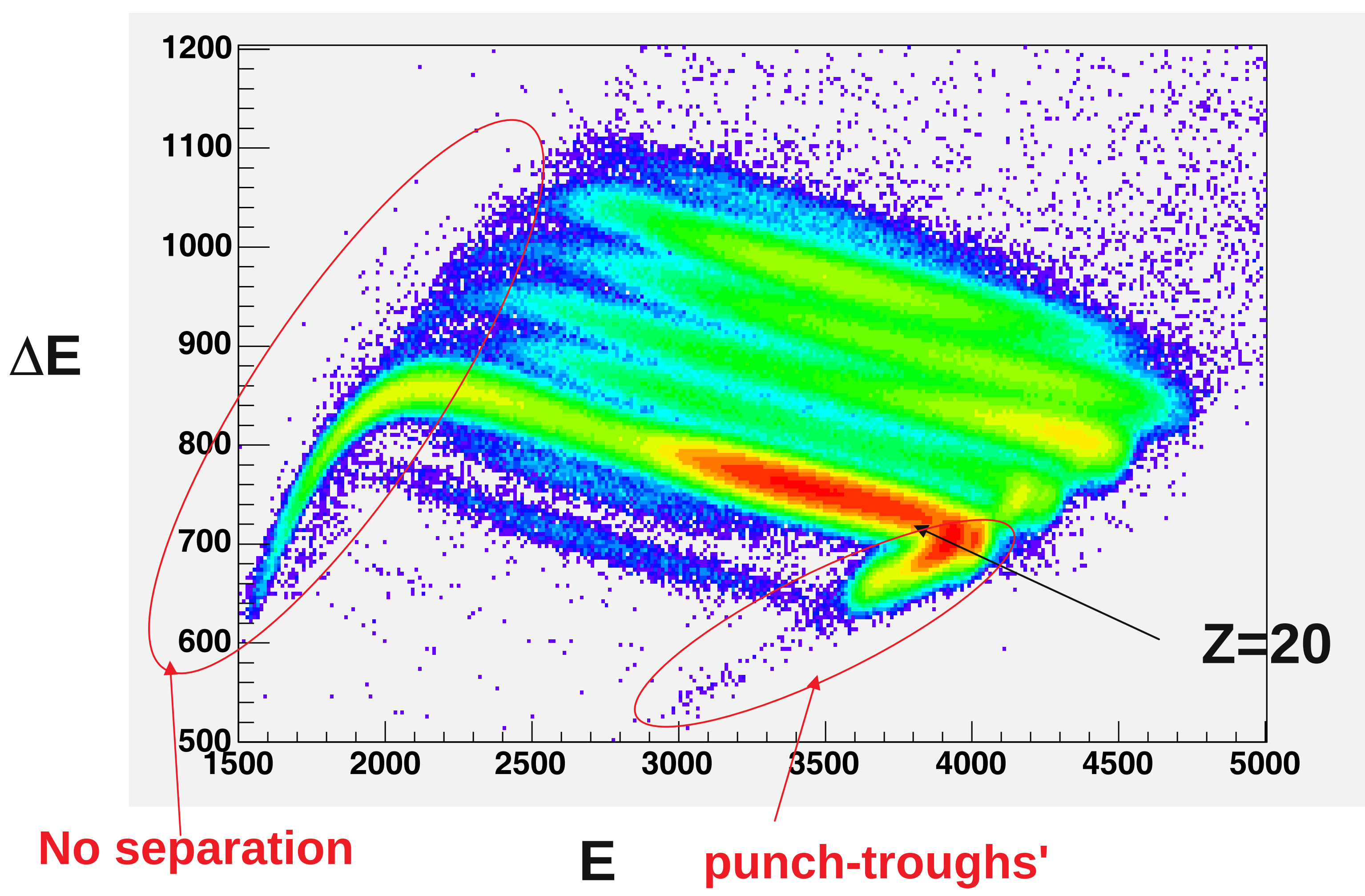

Range measurements:

Z-determination from range measurements

$$\frac{dE}{dx} = const \bullet \rho \frac{Z_{material}}{A_{material}} \bullet \frac{MZ_{ion}^{2}}{E} \bullet f(E)$$

Range ~ E^2 /(MZ^2)

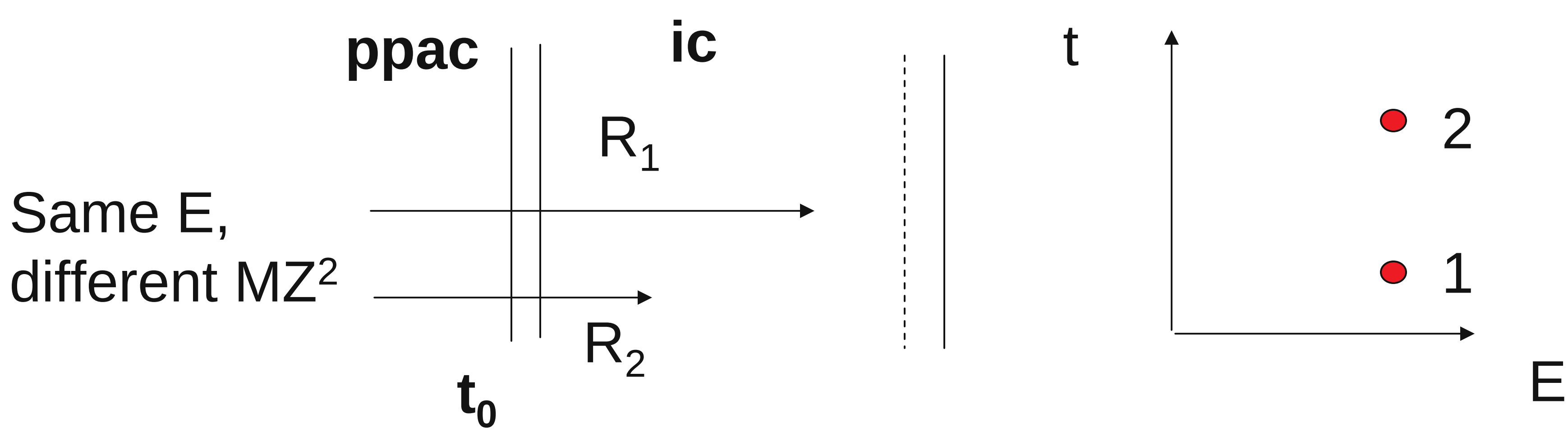

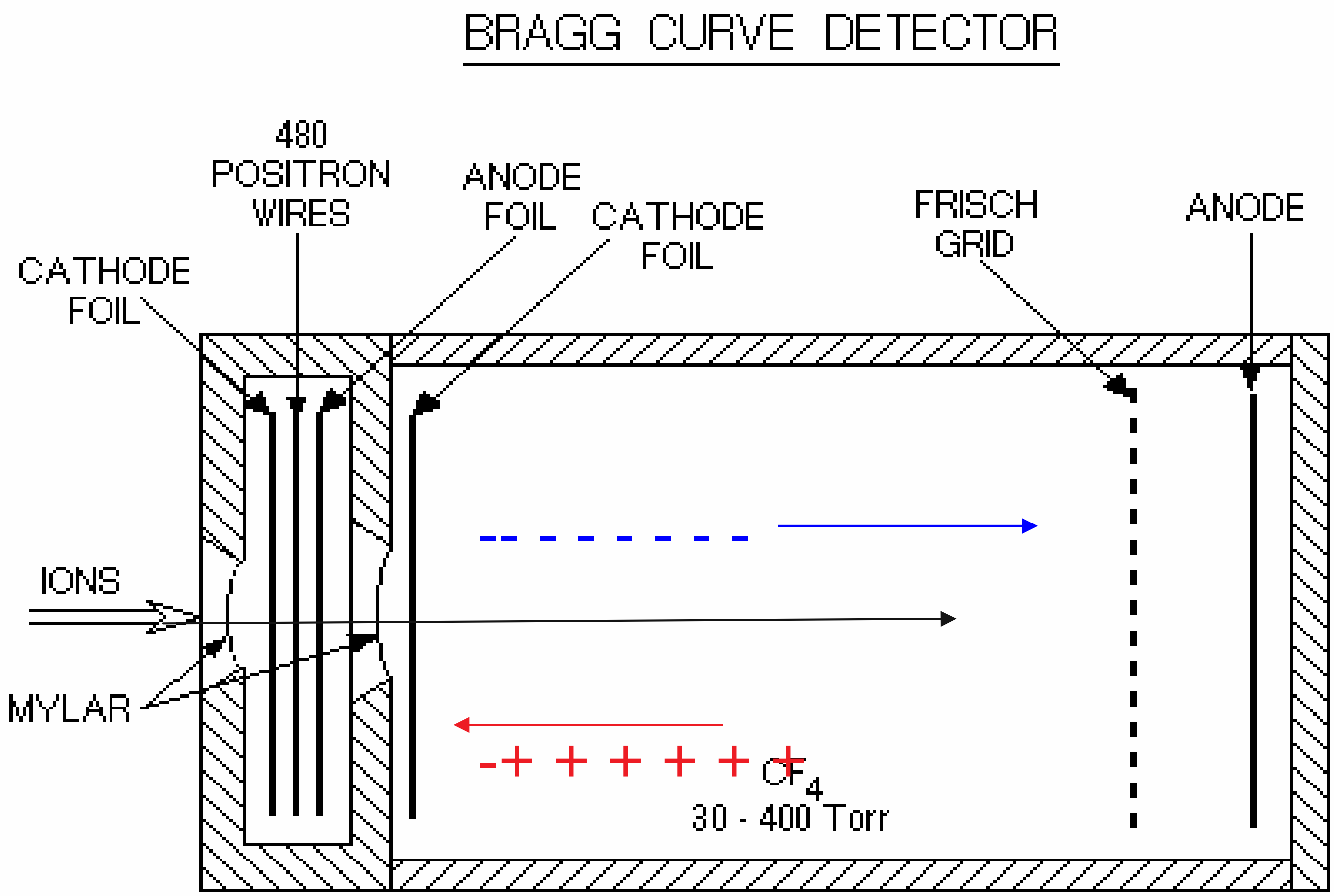

Cross section of Detector 1 available for the spectrographs.

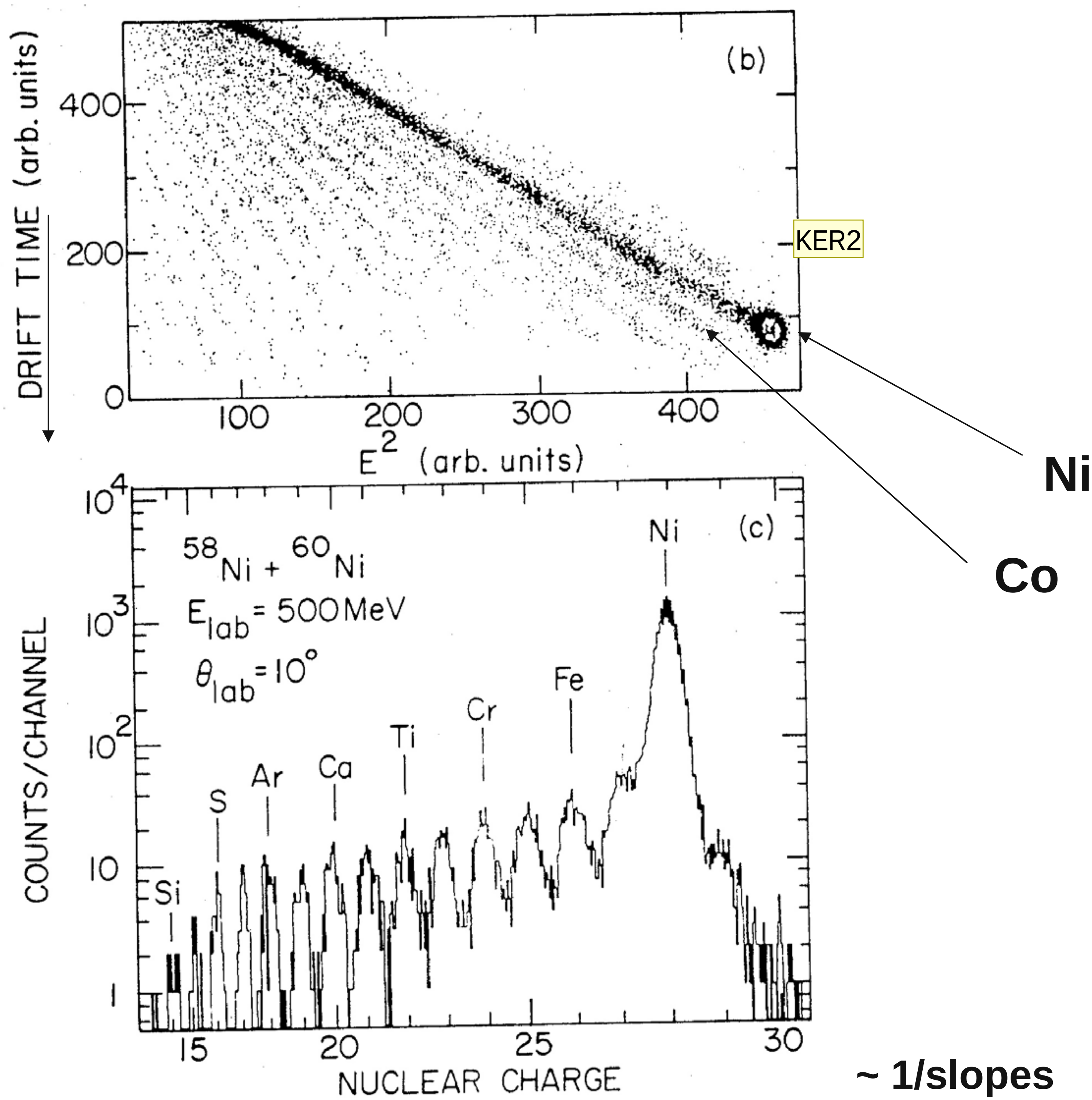
(b)
DRIFT TIME (arb. units)
400
200
0
100
200
300
400
E2 (arb. units)
KER2
Ni
Co
(c)
58Ni + 60Ni
Elab = 500 MeV
θlab = 10°
COUNTS/CHANNEL
Si
S
Ar
Ca
Ti
Cr
Fe
Ni
15
20
25
30
NUCLEAR CHARGE

~ 1/slopes

Slide 33

KER2 rehm, 2/12/2008

Advantages/disadvantages of $\Delta E/E$ and range techniques

- Works well at high energies
- Requires very homogeneous detector
- Difficult for slow particles (use ionization chamber)
- Need other Z-dependent process

Detection of characteristic X-rays

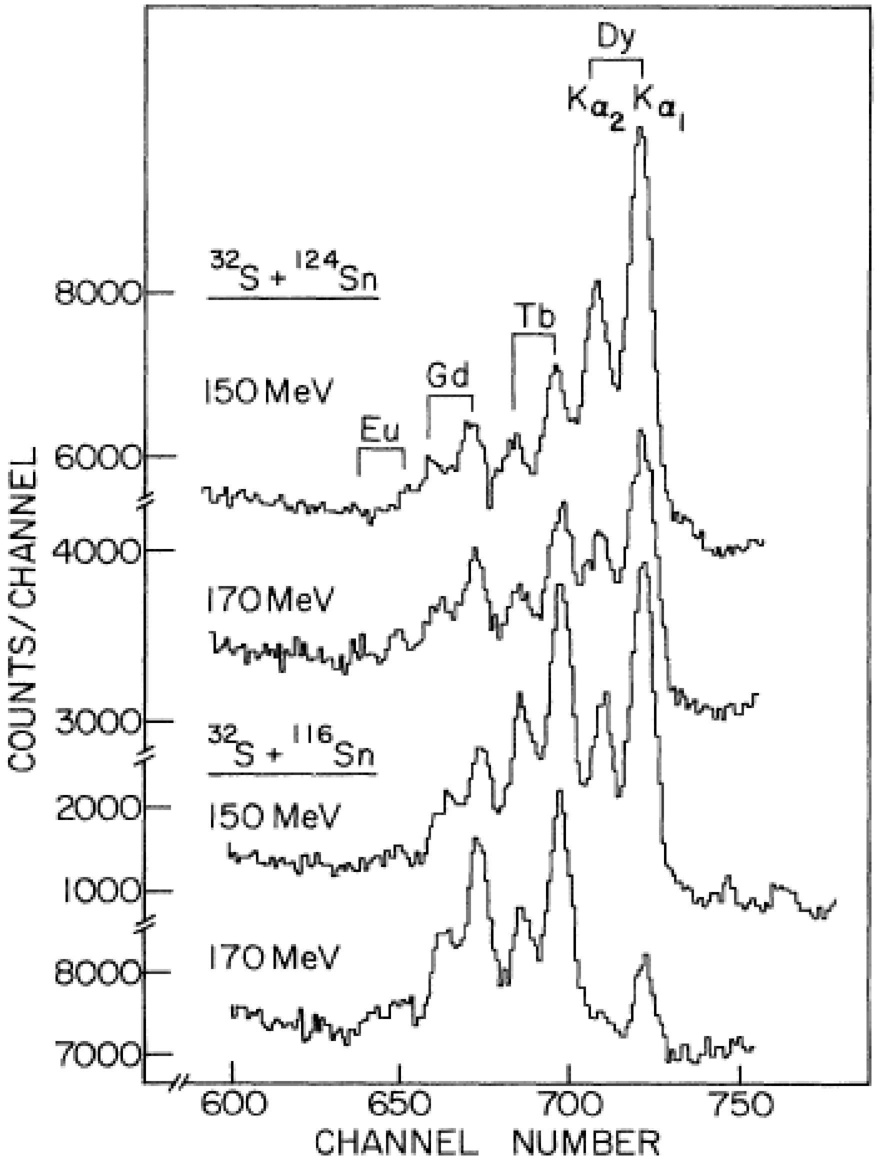

H. Ernst et al., PRC 29, 464(1984)

Efficiency!!!

X-ray production cross sections, multiplicities.

Gas-filled magnet technique

Principle

In a gas-filled magnet: $\bar{q} \approx \bar{v} Z^{\gamma} \bullet (1 + f(Z, v))$

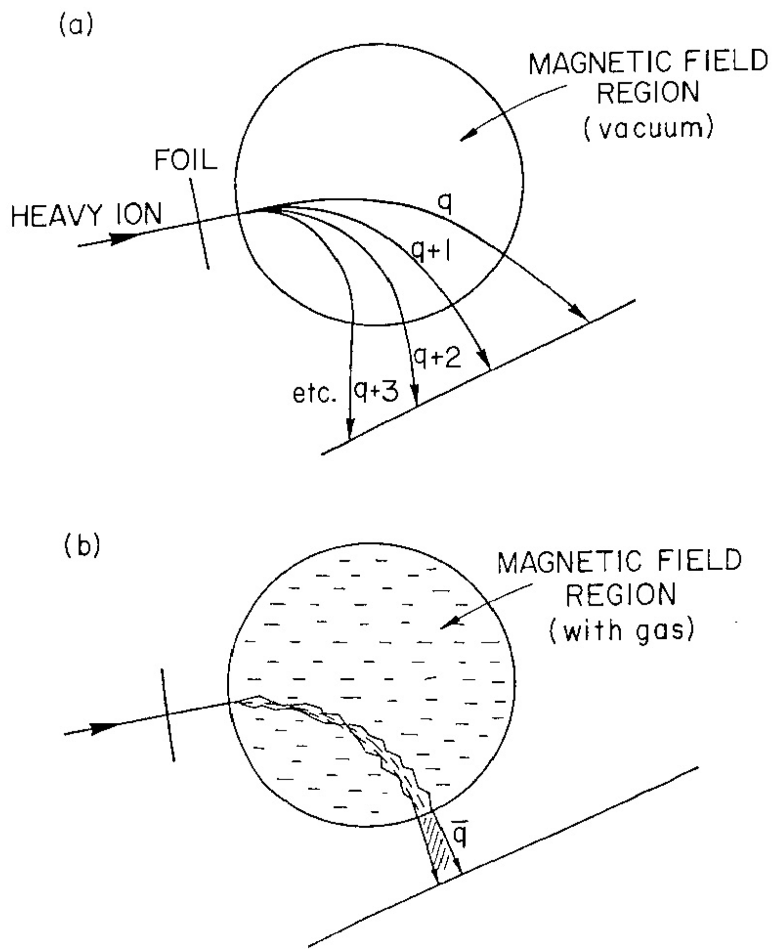

For magnetic rigidity Bρ:

$$B\rho = \frac{mv}{q} = \frac{m}{Z^{\gamma}}$$

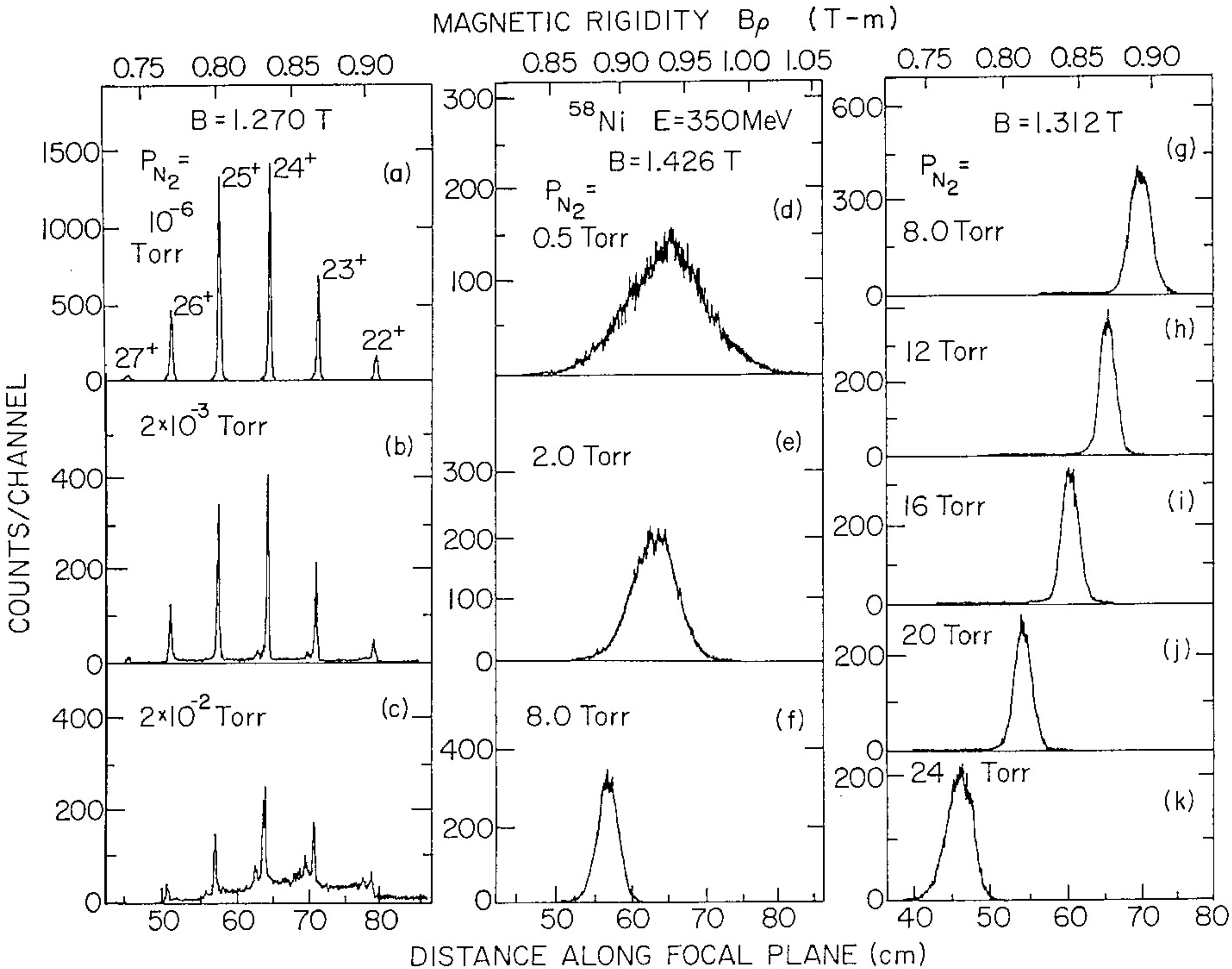

MAGNETIC RIGIDITY Bρ (T-m)
COUNTS/CHANNEL
DISTANCE ALONG FOCAL PLANE (cm)
B = 1.270 T
P_N2 = 10^-6 Torr
27+ 26+ 25+ 24+ 23+ 22+
(a)
2×10^-3 Torr
(b)
2×10^-2 Torr
(c)
58Ni E=350MeV
B=1.426 T
P_N2 = 0.5 Torr
(d)
2.0 Torr
(e)
8.0 Torr
(f)
B = 1.312 T
P_N2 = 8.0 Torr
(g)
12 Torr
(h)
16 Torr
(i)
20 Torr
(j)
24 Torr
(k)

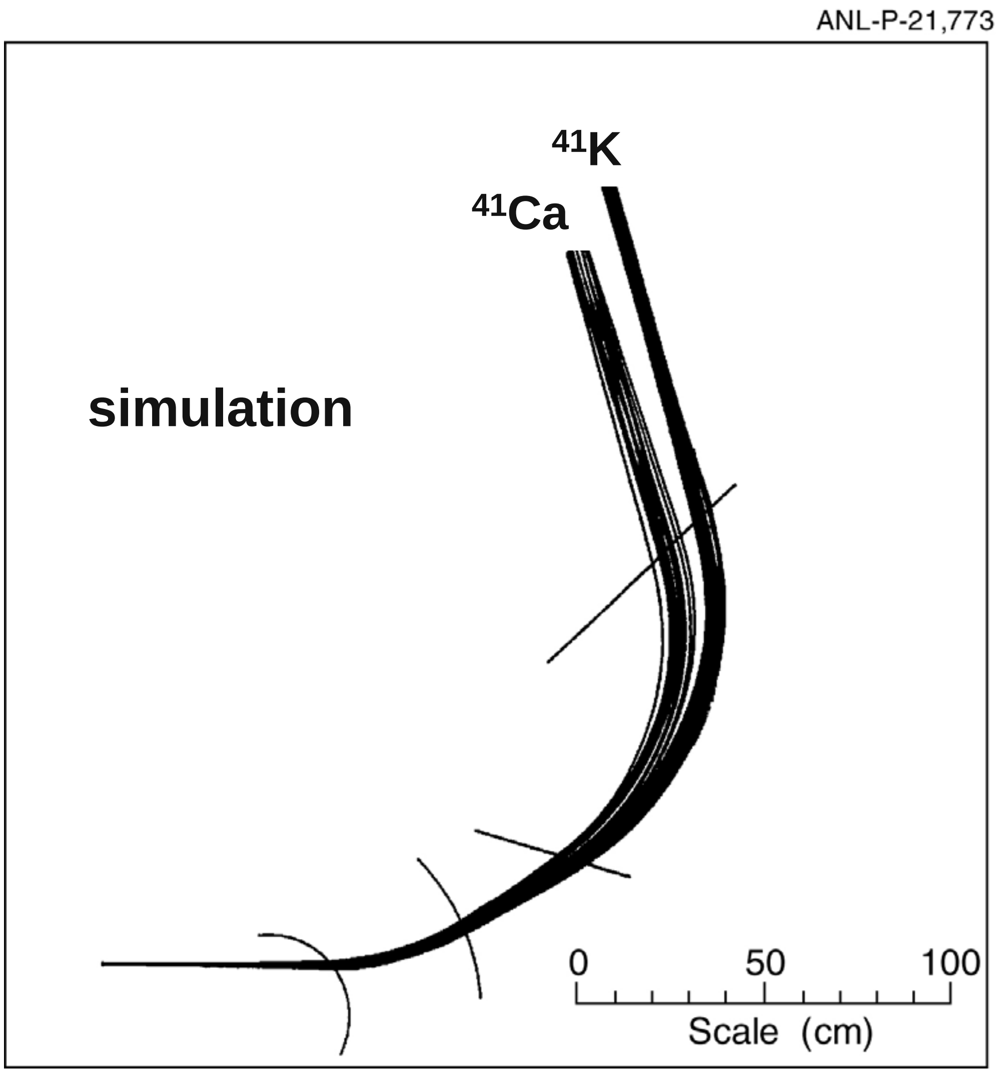
ANL-P-21,773
^{41}K
^{41}Ca
simulation
0
50
100
Scale (cm)

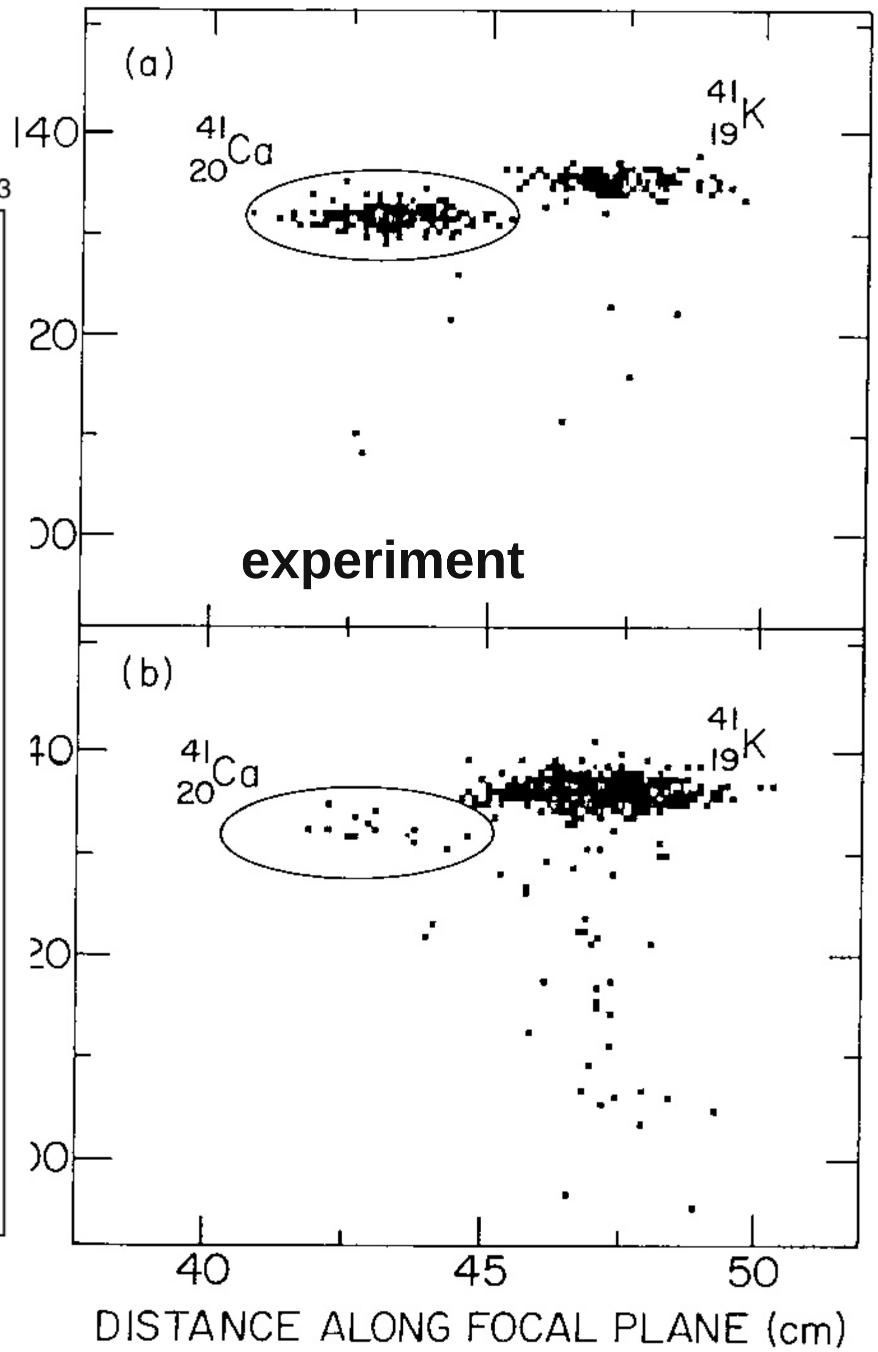
(a)
$^{41}_{20}$Ca
$^{41}_{19}$K
experiment
(b)
$^{41}_{20}$Ca
$^{41}_{19}$K
40
45
50
DISTANCE ALONG FOCAL PLANE (cm)

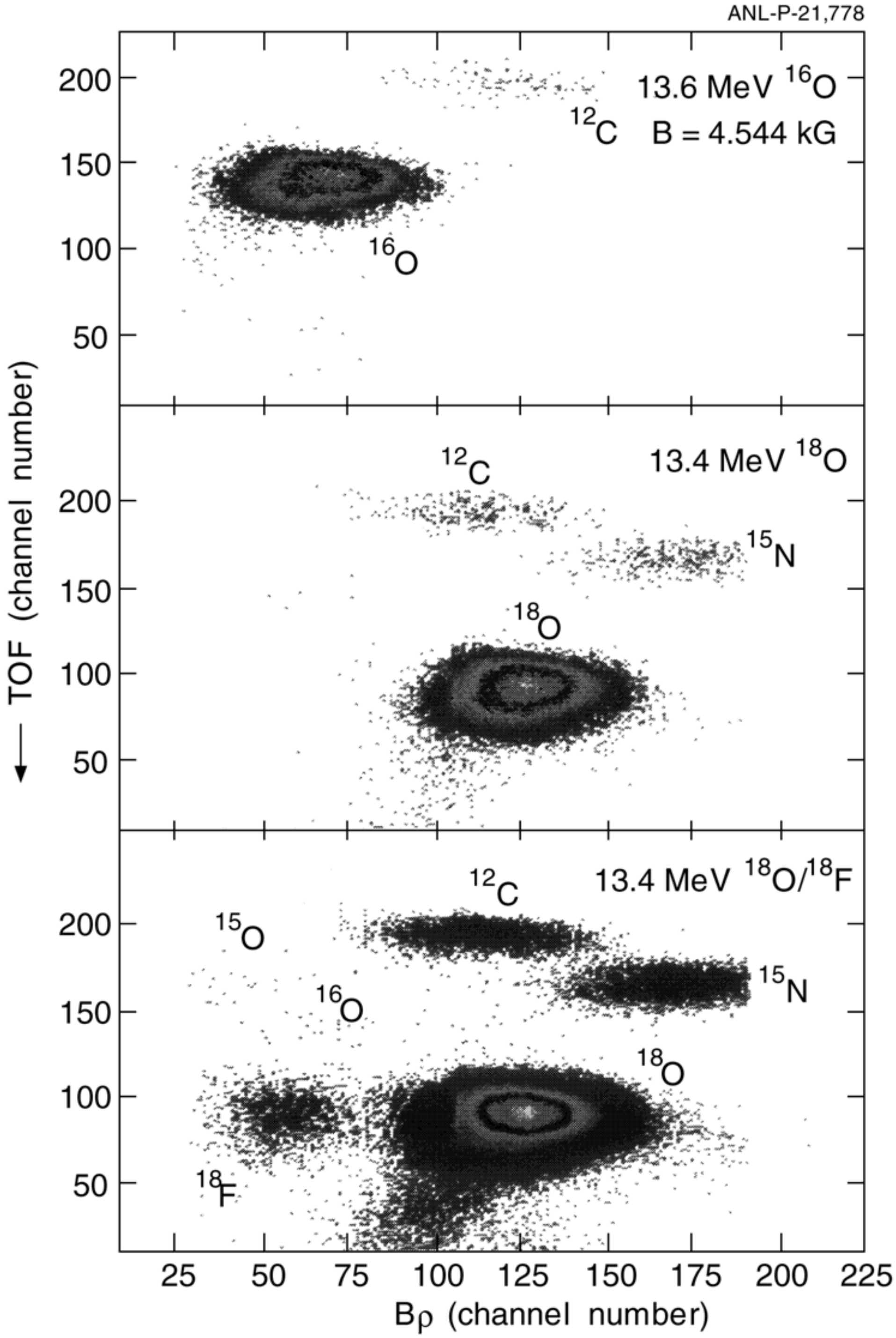

Particle separation with the gas-filled magnet technique at 600 keV/u

Works also for $^{58}Ni/^{58}Fe$ or $^{96}Ru/^{96}Zr$ with energies below 1 MeV/u, where ΔE-E techniques fail